A COMPUTATIONAL STUDY OF SINGLE AND DOUBLE STAGE HALL THRUSTERS

Kay Sullivan, Manuel Martínez-Sánchez, Oleg Batishchev and James Szabo

Massachusetts Institue of Technology
77 Massachusetts Avenue
Cambridge, MA 02139

Abstract

The numerical methods developed for the 2-D modeling of Hall thrusters are further refined, and results for the ceramic-lined single-stage P5 thruster at 300 and 500 volts are presented. The method is fully kinetic for all particles involved, and has been documented previously for a small TAL thruster [1]. Comparisons to experimental data and 1D simulations are made for verification of the current model, the anomalous diffusion model is tested, and various transport mechanisms are discussed. Performance of the P5 is well simulated by the code, although discrepancies in the spatial distributions suggest some adjustments still need to be made.

Introduction

To help understand the internal workings of Hall Thrusters MIT, together with NASA-Glenn and Busek, are developing fully kinetic simulations of several different engines. Previous papers presented successful simulations of the mini-TAL [1], and described a first round modeling of the SPT-type P5 [2]. After the single-stage SPT thruster is implemented, a sputtering module will be added, and a two-stage thruster will be modeled. When complete, the simulation will serve as both a research tool and a design aid.

This paper describes the latest developments of a full Particle-In-Cell simulation of the P5. We are continuing to refine our methods with improvements to the diffusion model. First, the current methods used in the simulation are stated. Second, results at 300V and 500V are presented, and third, some transport and modeling issues are discussed.

Simulation Method

This fully kinetic particle-in-cell simulation was originally developed by James Szabo for his Ph.D. thesis at MIT [3]. Szabo designed the code for the 50W mini-TAL designed by Khayms [3]. Vincent Blateau used this model to investigate high power operation of the mini-TAL [4]. Blateau later modified the code to simulate the P5 thruster built by Frank Gulczinski at Michigan [5]. The current methods used in the simulation are summarized here.

Basic Particle Motion

Three dimensions of velocity and two of position are modeled. The thruster is axisymmetric, therefore azimuthal motion is projected back into the radial-axial (z-r) plane. The simulation region is a 2D slice of the thruster starting at the centerline and encompassing the chamber and part of the plume. The cathode is not directly simulated.

Electrons and Ions are moved each iteration using a leapfrog method. The charged particles are moved a half time step in the electric field, then a full time step in the magnetic field, and then another half time step in the electric field. The time step is approximately one third of the electron plasma time or one third of the electron gyro time, whichever is smaller.

Collisions

After the electromagnetic motion is calculated, collisions are applied. First and second ionization of neutrals, electron-neutral scattering, electron-neutral excitation, ion-neutral scattering, ion-neutral charge exchange, second ionization of ions, and anomalous electron collisions are modeled. The anomalous collisions are used to model the additional Bohm diffusion observed in plasmas. Coulomb collisions were tested in the original model, but were found to have negligible effects and were turned off [3].

The probability of a collision is determined by an exponential decay model. The probability of a particle with collision frequency ν undergoing at least one collision in time dt is $P = 1 - e^{-\nu dt}$. A collision event occurs if a random number is less than the probability of a collision. The collisions frequency is calculated using the fast particle's velocity and collision cross-section and the slow particle density

interpolated to the fast particle's location. If a collision occurs, a second random number is compared to each type of collisions frequency, ionization, scattering, etc., to determine which type of collision is implemented.

Poisson Solver

The electric potential is found by solving Poisson's equation, $\nabla^2\phi = \frac{\rho}{\varepsilon_0}$, on a control volume around each grid node. Due to the higher mesh distortion in the P5, Blateau modified the solving algorithm to use an 8-sided polygon about each node as the control volume cross-section [6]. The TAL model used only a 4-sided polygon. The field is solved for the whole grid by using an iterative Successive-Over-Relaxation technique on the above conditions. At some boundary nodes the full set of equation does not need to be solved. At the anode the potential is the anode voltage. On the free space boundary, the potential is set to -10 or the normal electric field is set to zero, whichever results in the higher potential. At the dielectric walls, the electric field normal to the wall is also neglected.

Magnetic Field

Because the self-induced magnetic field is negligible compared to the applied field from a Hall thruster's coils, the simulation uses only a constant magnetic field. This field is precompiled using a Maxwell-type generator and interpolated to the simulation grid upon startup.

Numerical Tricks

To speed up the code, which currently takes a week to converge, three numerical tricks are used. First, superparticles are modeled instead of real particles. Each charged particle in the simulation actually represents N real ions or electrons. Simulated neutrals have variable sizes greater than or equal to one superparticle to account for the much higher neutral densities in the chamber. The superparticle size N is determined by the desired number of particles per cell, which is in turn based on computation time and statistics.

Second, the time and length scale of electromagnetic phenomena are modified by introducing an artificial permittivity γ. The artificial permittivity decreases the plasma frequency and increases the Debye length. However, the Debye length must remain smaller than about half the chamber for electromagnetic effects to occur on relatively the correct scale, and once the plasma time drops below the cyclotron time, no added benefit is gained.

Third, the heavy particle mass is reduced by a factor f. This increases the velocities of the heavy particles by $\sqrt{f}$, allowing ions to exit the simulation region in fewer time steps. In order to maintain the ion density and energy fluxes at their nominal values, the neutral mass flow, the ionization current, and collision cross-sections with heavy particles are also increased by $\sqrt{f}$.

Wall Sheath Fix

The sheath is determined self-constantly by accumulating the charges from impacting ion and electrons. Due to their higher-than-normal velocity but normal density, the ion number fluxes to the walls will be too high by the mass factor. This causes the sheath to weaken. Blateau identified that this problem was not important in the short-chambered TAL, but became a significant source of error in the P5 geometry [6]. He solves the problem by computing the difference between the theoretical and actual sheath magnitudes. Any electron with energy less than k times that difference is specularly reflected instead of being accommodating to the wall. The sheath potential is reduced by k, and a higher energy electron in the same region is impacted on the wall instead.

Cathode Model

The cathode is not included in the simulation region, therefore fluxes through the free space boundary must account for the injected electrons. The current cathode model was developed by Blateau [6]. Neutrality is maintained along the free space boundary by injecting electrons with a half-Maxwellian distribution in cells with positive potential. Boundary cells with negative potential are left alone. Electrons hitting the upper free space boundary are reflected with an energy loss to simulate collisions with the walls at the end of the magnetic field lines.

Conditions for Current Runs

The current grid has 88x96 cells, a cell length of approximately 0.8 mm, and a cell volume of 0.216 cm^3. A mass factor of 1000 and an artificial permittivity of 40, result in a maximum artificial Debye length of approximately 1 mm. The maximum electron plasma frequency and Larmor frequency are both on the order of 10^8 Hz, resulting in a time step of approximately 10^{-10} s per iteration. With this time step and mass factor, neutrals take approximately 140,000 iterations to clear the chamber.

Changes to Diffusion Model

In [2], Blateau used a direct random walk method for simulating anomalous diffusion. As reported there, the simulation only converged for very low values of diffusion. Performance characteristics for that case were within 15% of experimental data, but the electron temperature, in particular, was surprisingly high. A 2D test of the diffusion model, however, showed that it was not producing mobility, and that it artificially heated the electrons to temperatures as high as 100eV. Re-examination of the original diffusion model showed that it was capable of producing equal to or greater than the expected mobility. Results described here use the original anomalous diffusion model with a Hall parameter of 400. A more detailed exploration of the diffusion issue is presented in the discussion section.

Simulation Results

We tested the simulation of the P5 at 3kW and 5kW. Experimental data from James Haas [7] was used to check results. Haas took extensive measurements at 3kW and also gave performance data for 5kW operation. All settings except the anode voltage, maximum magnetic field, and neutral flow rate were the same between the runs. A comparison of the simulated and experimental performance data is in Table 1. All figures for this section are included at the end of this document.

Table 1 - Summary of Code and Experimental Thruster Performance

	3kW PIC	3kW Experimental	5kW PIC	5kw Experimental
Maximum B	290 G	250 G	360 G	360 G
Anode Voltage	300 V	300 V	500 V	500 V
Anode Current	7.5 A	10 A	7.4 A	10 A
Mass Flow Rate	11.41 mg/s	10.74 mg/s	10.83 mg/s	10.83 mg/s
Thrust	180 mN	180 mN	226 mN	240 mN
ISP	1600 s	1650 s	2210 s	2300 s
Efficiency	0.63	0.48	0.64	0.57
Oscillation Freq	6.5 kHz	N/A	11.7 kHz	11 kHz

The code correctly predicts thrust and specific impulse, but under predicts the anode current by 25% at both power settings. The main oscillation frequency observed in the plasma, after being corrected for the artificial permittivity, matches the anode current oscillation frequency observed by Haas.

A more detailed look into the thruster operation shows that most phenomena are concentrated closer to the anode and over a larger region than expected from the experimental results. Plasma potential simulations, Figure 12 and Figure 13, show a gradual drop towards the anode, while the probe data, Figure 7, shows a high potential filling most of the chamber and dropping suddenly near the chamber exit. Interestingly, at 3kW the simulated and measured potentials both exhibit a bowing out near the center of the chamber exit that is much weaker at other voltages.

The average electron temperatures in the chamber, shown in Figure 14 and Figure 15, are lower than those observed experimentally, Figure 6, by about 10eV, but have approximately the correct shape and concentration. Both the measured and simulated temperatures are concentrated between 20 and 35 mm down the chamber, although the simulated results are slightly shifted towards the anode. The ion density peak, Figure 8 and Figure 9, is of the right magnitude, but is severely shifted towards the anode compared to the probe data in Figure 5.

The simulated ion density profile is also much wider than measured experimentally. Haas shows the ion density peaking at the channel exit and almost immediately dropping off upstream. The simulation results show medium to high densities filling the chamber in a fish-like shape. Figure 16 shows that the peak ionization is right on top of the anode. While this is consistent with the density peak near the anode, the peak ionization region should be near the end of the chamber in the area of maximum magnetic field.

Effect of Increased Voltage

The results at 500V very closely resemble those at 300V. The ion density peak is smaller and closer to the anode. The double ion distribution in the 500V case is of the same magnitude but more spread out than the 300V distribution. The plasma potential profile is identical except for the bump at the end of the chamber. The electron temperature is found closer to the outer dielectric wall, and as expected, has increased with the anode voltage.

Evolution of density and temperature

Following the operation of the thruster over time shows deep oscillations at the plasma frequency. The magnitude of these oscillations shrinks as the anomalous diffusion is reduced and becomes more sever as the anomalous diffusion is increased. Oscillations also become less sever with higher voltage. Figure 17 through Figure 20 show the 500V ion density profiles at the half-way-to-maximum, maximum, half-way-to-minimum, and minimum current peaks. When rising, the ions form the fish-shape seen in the time averages. As the current falls, the ions become less concentrated, ending in isolated patches of ions at time of minimum current. The electron temperature, in Figure 21 through Figure 24, is out of phase from the ion density by a quarter cycle. When the current and ion density is rising, the electron temperature is at a minimum. When the current is falling, the electron temperature is at a maximum. The temperature peak approximately corresponds to the axial location of peak magnetic field magnitude. Interestingly, the temperature in the plume decreases as the temperature in the chamber increases.

Discussion

Model for mobility and diffusion

Anomalous diffusion is modeled via a modification of Bohm's diffusion formula

$$D_{ano} = \frac{kT_e}{\beta' eB} \qquad (1)$$

where the "anomalous Hall parameter" β' is chosen parametrically. Mobility is then derived through the Einstein relation. In order to obtain these effects in the simulation, the current procedure is to execute additional collisions over and above the number indicated by the existing densities and cross sections. The frequency ν_{ano} of these extra collisions follows from equating (1) to the classical expression (at low collisionality)

$$D_{class} = \frac{kT_e}{m_e} \frac{\nu_{ano}}{\omega_c^2} \qquad (2)$$

The originally recommended β' parameter is 16, but other researchers [3], [8] have found that best agreement with performance data in Hall thrusters requires a larger value, of the order of 64. This value is also supported by direct simulation results presented by Batishchev in a parallel paper [9]. In our numerical work on the P5 thruster, we have found that even these larger values of β' (which imply a reduced level of anomalous mobility) are insufficient, and that best performance and oscillation results require $\beta' \approx 200 - 400$. Figure 1 shows computed current vs. time for a series of test runs using different β' values. It can be seen that lower values of β' normally lead to either divergence or extinction of the discharge and to clearly inaccurate average current in any case.

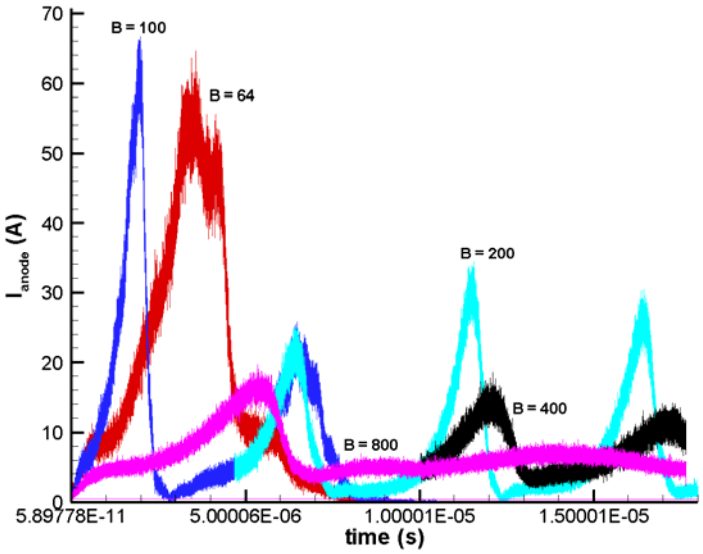

Figure 1 - Anode Current versus Time for Various Hall Parameters

In order to investigate this effect, a series of test cases were devised in which the plasma geometry of the P5 was retained, but most of the dynamics were suppressed. Heavy particles were frozen in place, the $\vec{E}$ field was fixed as a purely axial and uniform field, and the $\vec{B}$ field was made uniform and radial. A large number of electrons were tracked in these fields, and their mean axial velocities recorded after many collisions and many gyrations. The results of these tests were at first surprising, in that the implied electron cross-field mobility was typically several times greater than could be calculated from Eq(2) plus Einstein's relationship. Upon closer inspection, it was found that a significant, sometimes dominant, contribution to the axial displacement was due to secondary electron emission from the ceramic walls. Since the secondary electron is emitted in a random direction, there is an average displacement against the $\vec{E}$ field associated with these events. Figure 2 shows a portion of a trajectory in which this effect is captured. When the secondary emission was also artificially suppressed, the computed mobility agreed with the calculation based on collision frequency.

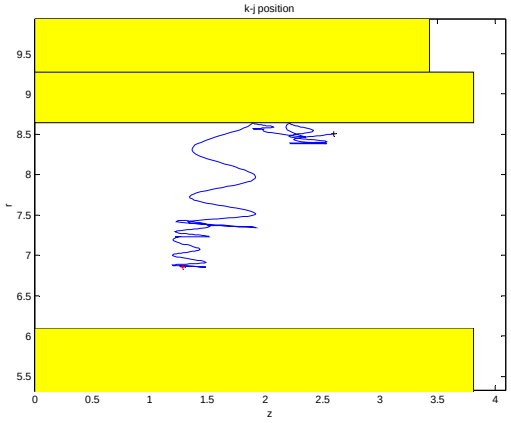

Figure 2 – Primary to Secondary Electron Trajectory, inverted electric field

This "wall conductivity" is, of course, not a new phenomenon, and its existence, in association with secondary emission or with diffuse scattering from walls has been postulated in the Russian literature for many years. However, based on estimates derived from 1D modeling work [10] we had not expected it to be

significant, except perhaps locally in the highest electron temperature region. Unfortunately, we have not yet been able to verify that the same effect is indeed occurring in the full simulations. In principle, a much smaller number of electrons should be reaching the walls when the full sheath potential is allowed to develop. However, a number of numerical procedures have been introduced in our model in order to deal with the artificially increased ion speeds (reduced mass ions) without distorting the particle or energy fluxes, and we suspect that, as an unwanted side effect, these may have introduced additional scattering. If that were the case, it would explain why we have been forced to strongly reduce the bulk anomalous diffusivity and mobility. It would also indicate a possible problem in the outside portions of the domain: the reduced bulk mobility cannot be compensated there by the extra wall mobility, and cathode electrons may be unduly inhibited from reaching the discharge region.

Axial extent of the discharge

It was noted in the Results sections that the computed time-averaged distribution of plasma density is much wider axially than indicated by data from the "sting" probe. We have noticed a similar discrepancy in other computations of various types. The work of N. Warner et al. [11], for the BHT 1000 thruster using the same code also indicates a computational widening in comparison to probe-derived data, although the effect is not as marked. For the same thruster, Szabo et al [12] finds that the ionization oscillation frequency varies with voltage as predicted by the "predator-prey" model, but is generally lower, which could be due to a computed ionization layer that is too wide. A completely independent model, the 1D model of Ahedo et al [8], also predicts definitely wider plasma distributions. Figure 3 and Figure 4 compare those results with the radial and temporal average of results from our code. Although detailed agreement is lacking, the width feature is common to both results. Finally, the 1D model of Rostler [12], which uses completely independent assumptions, does predict an even wider plasma.

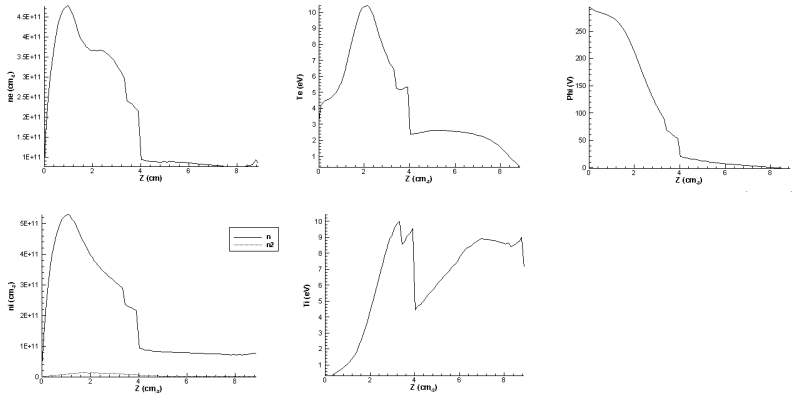

Figure 3 - 1D Averages of P5 PIC Simulation, discontinuities due to increases in averaging area

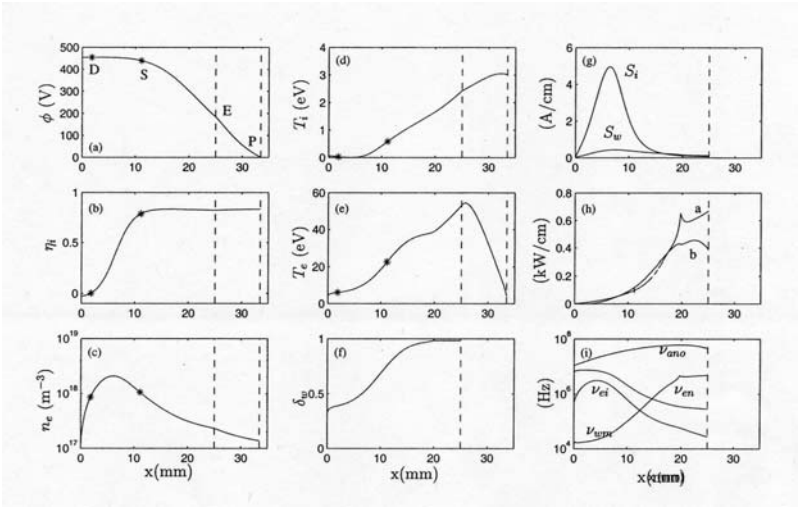

Figure 4 - 1D Averages for the SPT-100 from [8]

In fact, the 1D theory [8] provides a strong argument in favor a linear decay of electron pressure $P_e = n_e kT_e$ between the ionization region and the anode, the so-called "diffusion region". Including the fact that T_e is significantly lower near the anode than in the ionization layer, one can see why the n_e profile would adopt the characteristic "whale hump" shape visible in Figure 3. The very strong reduction in n_e on the anode side of the ionization layer in the P5 probe data is clearly at variance with this argument.

This apparent systematic discrepancy will need to be explained and removed in future work. At this point we can only speculate on possible explanations:

(a) The axial electron mobility being used in all models is still too high. In general, this hypothesis would seem unlikely, given the amount of indirect evidence (based on performance) for the values commonly used. Alternatively, the anomalous mobility might, for some reason, be lowest precisely in the ionization region, but again this is not easy to rationalize.

(b) There are unaccounted for mechanisms enhancing the ionization rate. To our knowledge, all models use ionization rates that assume direct ionization from the ground state through electron collisions. Among the candidate additional mechanisms, we can list two-step ionization mediated by a long-lived excited state (probably a metastable state), overpopulation of upper states due to trapping of resonant UV radiation, and heavy-heavy collisional ionization (although this is more likely in the plume than in the ionization layer).

(c) There could be reasons why probes tend to underestimate the electron density near the anode, although we could not ourselves identify any systematic reason for this.

Conclusions

We have presented here computational results based on a full PIC model for the performance and plasma dynamics of a ceramic-lined P5 thruster. The results are encouraging and give reasonable agreement with measurement as to performance and oscillation frequency. However, there are differences of detail in the spatial distribution of plasma parameters that may indicate systematic modeling deficiencies. These are discussed and some hypothesis are formulated that will form the basis for additional research, now that a working tool is at hand.

Figures

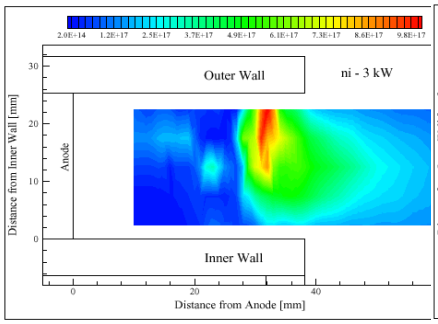

Figure 5 - Experimental Ion Density 3kW (m^{-3})

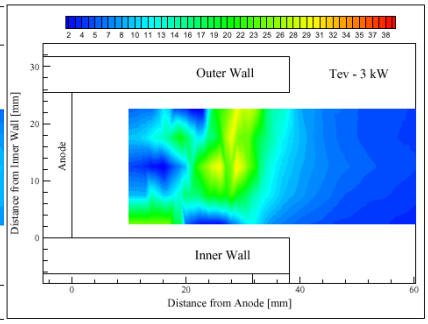

Figure 6 - Experimental Electron Temperature 3kW(m^{-3})

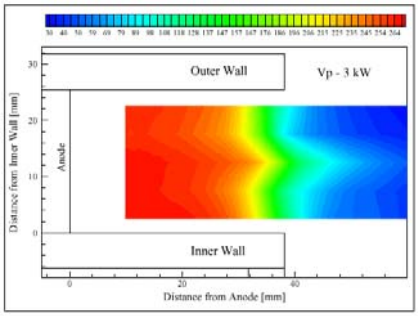

Figure 7 - Experimental Plasma Potential 3kW (m^{-3})

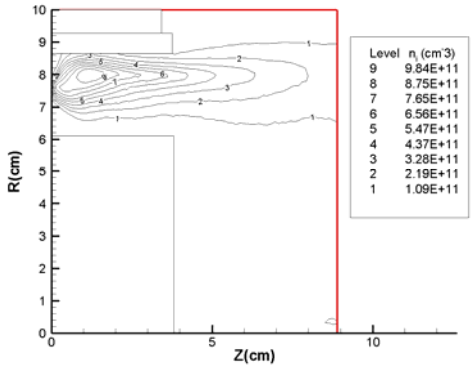

Figure 8 - Simulated Ion Density 3kW

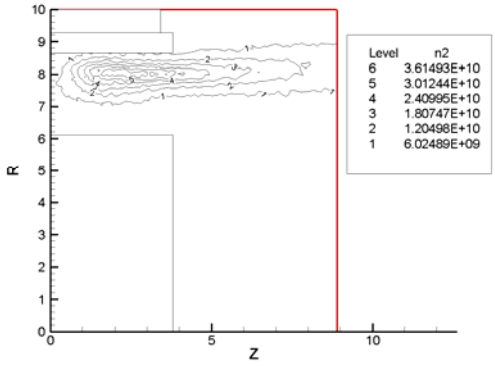

Figure 10 - Double Ion Density 3kW (cm^{-3})

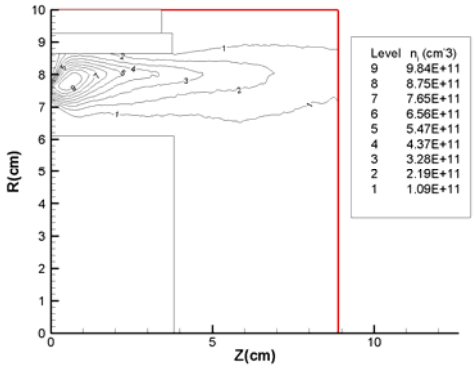

Figure 9 - Simulated Ion Density 5kW

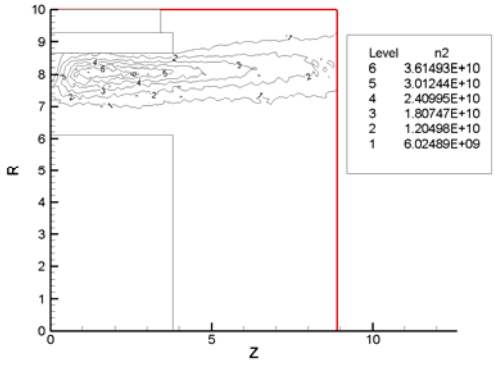

Figure 11 - Double Ion Density 5kW

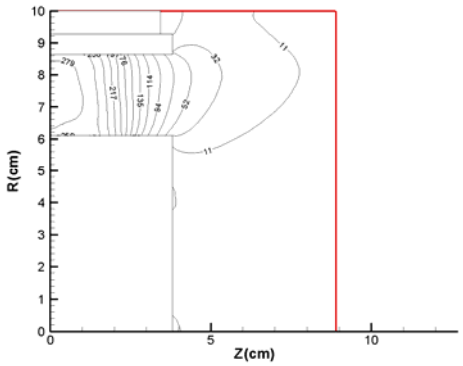

Figure 12 - Plasma Potential 3kW

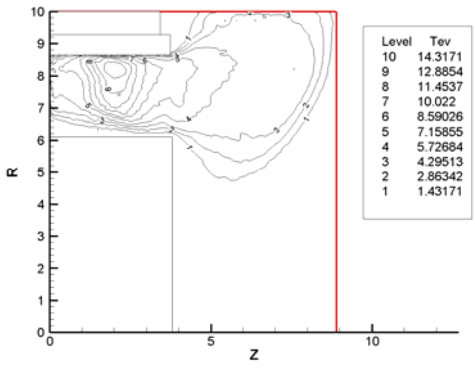

Figure 14 - Electron Temperature 3kW

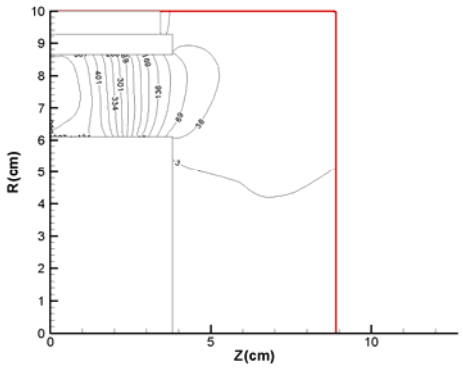

Figure 13 - Plasma Potential 5kW

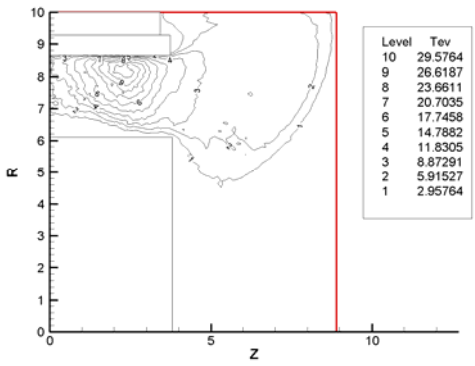

Figure 15 - Electron Temperature 5kW

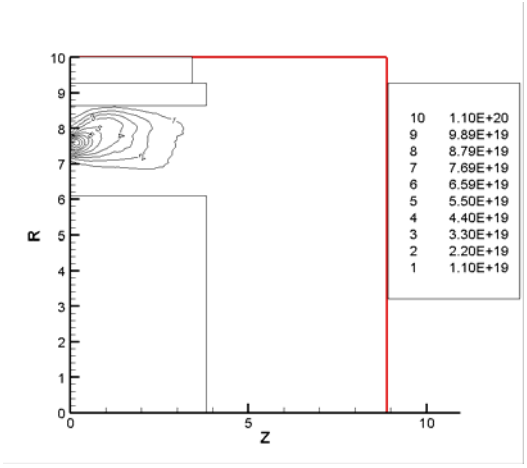

Figure 16 - Xe-Xe+ rate 3kW (Hz)

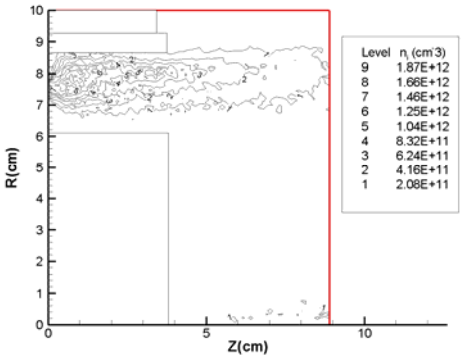

Figure 17 - Rising Current Ion Density 500V

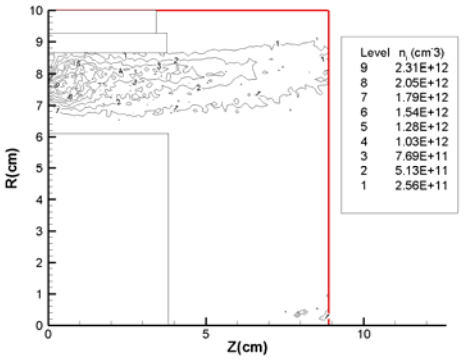

Figure 18 - Maximum Current Ion Density 500V

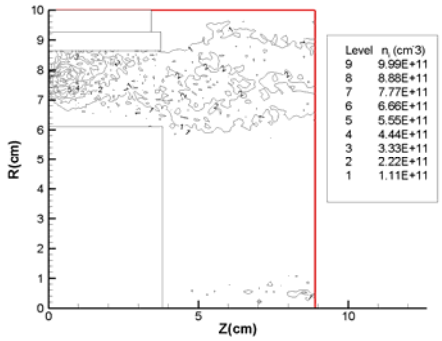

Figure 19 - Falling Current Ion Density 500V

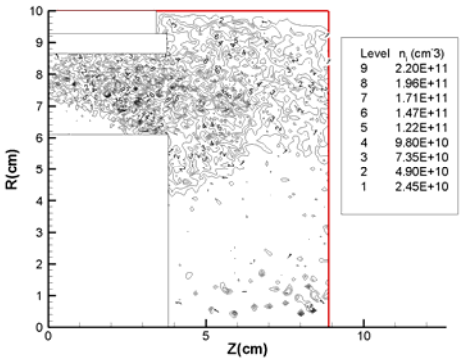

Figure 20 - Minimum Current Ion Density 500V

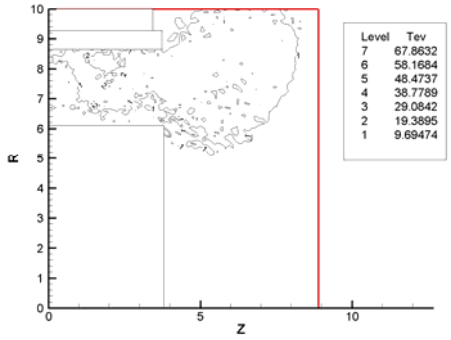

Figure 21 - Rising Current Electron Temperature 500V

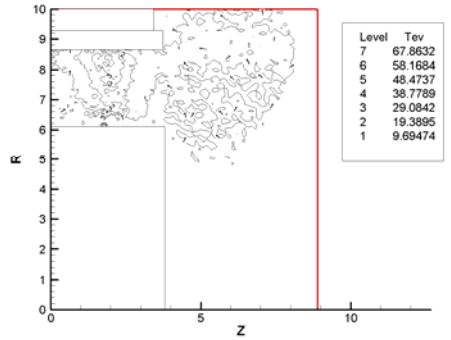

Figure 22 - Maximum Current Electron Temperature 500V

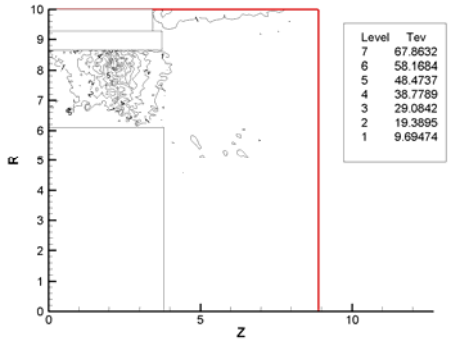

Figure 23 - Falling Current Electron Temperature 500V

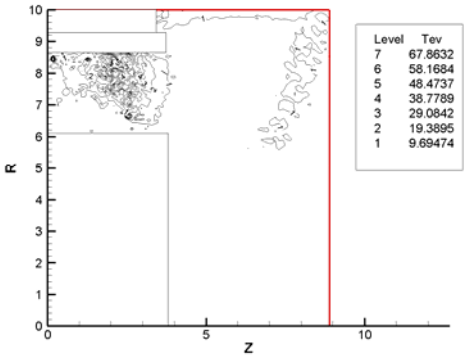

Figure 24 - Minimum Current Electron Temperature 500V

References

[1] Blateau, V., Martinez-Sanchez, M., Batishchev, O., Szabo, J., "*PIC Simulation of High Specific Impulse Hall Effect Thruster*", IEPC-01-037, 27 International Electric Propulsion Conference, Pasadena, CA, October 15-19-2001.

[2] Blateau, V., Martinez-Sanchez, M., Batishchev, O., "*A Computational Study of Internal Physical Effects in a Hall Thruster*", AIAA-2002-4105, Joint Propulsion Conference, July 7-10, 2002, Indianapolis, Indiana.

[3] Szabo, J.J., "*Fully Kinetic Numerical Modeling of a Plasma Thruster*", Ph.D. Thesis, MIT, 2001.

[4] Khayms, V. "*Preliminary experimental evaluation of a miniaturized Hall thruster*", IEPC-97-077, International Electric Propulsion conference, Pasadena, CA, October 15-19, 2001.

[5] Gulczinski, F.S., "*Examination of the Structure and Evolution of Ion Energy Properties of a 5 kW Class Laboratory Hall Effect Thruster at Various Operational Conditions*", Ph.D. Dissertation, University of Michigan, 1999.

[6] Blateau, V., "*PIC Simulation of a Ceramic-lined Hall-effect Thruster*", M.S. Thesis, MIT, 2002.

[7] Haas, J.M., "*Low-perturbation Interrogation of the Internal and Near-field Plasma Structure of a Hall Thruster Using a High-Speed Probe Positioning System*", Ph.D. Dissertation, University of Michigan, 2001.

[8] Ahedo, E., Gallardo, J.M., Martinez-Sanchez, M., "*A model of the Hall thruster discharge with the effects of the interaction with the lateral walls*".

[9] Batishchev, O., and Martinez-Sanchez, M., "*Charged particles transport in the Hall effect thruster"*, 2003 International Electric Propulsion Conference, March 17-21, 2003, Toulouse, France, IEPC-2003-188.

[10] Ahedo, E., Martinez Cerezo, P., Martinez-Sanchez, M., "*Model of Plasma-Wall Interaction Effects in a Hall Thruster*", Joint Propulsion Conference, July 8-11, 2001, Salt Lake City, UT, AIAA-2001-3323.

[11] N. Warner, J. Szabo, M. Martinez-Sanchez, "*Characterization of a High Specific Impulse Hall Thruster Using Electrostatic Probes*," 2003 International Electric Propulsion Conference, March 17-21, 2003, Toulouse, France, IEPC-2003-82.

[12] Szabo, J., Rostler, P., McElhinney, S., Warner, N., "*One and Two Dimensional Modeling of the BHT-1000*", 2003 International Electric Propulsion Conference, March 17-21, 2003, Toulouse, France IEPC-2003-231.